Fabrication of Boehmite Nanofiber Internally-Reinforced Resorcinol-Formaldehyde Macroporous Monoliths for Heat/Flame Protection

*Gen Hayase**

Frontier Research Institute for Interdisciplinary Sciences, Tohoku University, 6-3 Aramaki-aza Aoba, Aoba-ku, Sendai 980-8578, Japan.

KEYWORDS. macroporous monoliths, nanofibers, fiber-reinforced materials, composites, resorcinol-formaldehyde, organic-inorganic hybrids

ABSTRACT. By distributing boehmite nanofibers to a resorcinol-formaldehyde (RF) skeletal phase formed by phase separation in an aqueous sol, composite macroporous monoliths have been produced by performing gelation, aging, and drying processes at 60 °C. In the nanofiber reinforced structure, boehmite nanofiber is arranged in parallel within the RF skeleton and showed high Young's modulus against uniaxial compression for their bulk density. These materials can be expected to be applied to heat/flame protection materials using their heat insulating properties and high flame resistance.

Macroporous monoliths composed of ceramics, organic polymers, and natural products have long been used for various applications.[1] The macroscopic physical properties of these materials have led to their use for heat insulation, sound absorption, and cushioning. The utility of macroporous monoliths as catalysts, battery materials, separation media, and small sensors are currently being investigated.[2] Unlike

powders or thin films, porous monoliths have a three-dimensional macroscopic structure. The controlled alteration of the structure and surface of porous monoliths allows the controlled alteration of physical properties and is an important area of research in both academia and industry. Increasing interest in energy conservation, the miniaturization of computer equipment, and the growth of private space industries are driving the need for high-performance heat insulating and shielding materials. This has led to increased research on porous materials due to their thermal insulation properties. In general, porous monoliths have a lower bulk density and finer structure than other materials, giving rise to attractive characteristic physical properties but also decreased mechanical strength.[2-3]

Various studies have focused on increasing the mechanical strength of low-bulk-density porous monoliths. For silica aerogels, several groups have reported that structures with surface modification of polymers have high strength and bendability, and some have already been commercialized in some applications.[4-6] Methylsilsesquioxane transparent aerogels ($CH_3SiO_{1.5}$) do not collapse when deformed 50–80% by uniaxial compression due to their elasticity and show superinsulating properties.[7-8] The thermal conductivity of these materials is below 15 mW m^{-1} K^{-1}, but they are fragile when subjected to bending and twisting, preventing their practical use. Flexible macroporous silicone materials "marshmallow-like gels" have a thermal conductivity of around 30 mW m^{-1} K^{-1} but their flexibility and environment resistance make their use practical.[9-10] Such materials can be used as "simple dry shippers" for storing frozen embryos and tissues at −150 °C or lower by having them absorb liquid nitrogen.[11] However, they are fragile when subjected to tension and friction. Moreover, in the improvement of mechanical properties focusing on elasticity and flexibility, the application purpose is limited. It is also important to study how to fabricate a strong structure that is difficult to deform. Improving the mechanical properties of porous monoliths for a wide application requires the design of composite materials whose microstructures are resistant to collapse. For example, the composition and morphology of the microstructure can be optimized by polymer modification of the skeleton and fiber reinforcement of the exterior of the material. Fiber reinforced plastic (FRP) is used as a structural material for aircraft and vehicles and as a building material and exhibits excellent mechanical properties due to the impregnation

and integration of resin with glass, carbon, or ceramic fibers. The excellent mechanical properties of FRP cannot be obtained by using plastics alone. Conventional fiber-composite porous monoliths with improved strength contain fibers outside the main skeleton or are covered with spherical particle aggregates.[12-15] Preparing such monoliths with increased strength without coarsening the microstructure and sacrificing other physical properties is challenging. Furthermore, the microstructure is reinforced by using nanofibers, but these fine fibers tend to form a bundle structure and are thus difficult to handle. If nanofibers can be used to reinforce microstructures from the inside, it becomes possible to produce strong monoliths.

We have produced porous monoliths by using boehmite nanofibers containing aluminum oxide hydroxide (AlOOH).[16-17] Those ceramic nanofibers have a high aspect ratio (4 nm average diameter, 1.2 μm average length) and show high dispersibility, which stabilizes over several months in acetic acid aqueous solution.[18] However, these nanofibers can quickly aggregate and gel upon changing the pH or adding a phosphoric acid compound.[16] Obtained monoliths by drying the wet gels show unique properties such as ultralow bulk density, transparency and ultralow refractive index, due to the structure consisting of dilute and well-dispersed nanofibers. In 2016, we reported a simple method for the generation of low-bulk-density porous monoliths by adding a tri-functional silicon alkoxide to a boehmite nanofiber dispersion under acidic conditions.[19] The alkoxide undergoes hydrolysis/polycondensation under acidic conditions to form silsesquioxane that covers each boehmite nanofiber and at the same time bonds the fibers together. Consequently, monoliths consisting of a rod-like skeleton with a diameter of several tens of nanometers can be obtained with good reproducibility. The mechanism of formation indicates that the skeleton has a core-shell-type structure in which boehmite nanofiber are surrounded by silsesquioxane, providing a material with excellent mechanical strength. This low-bulk-density boehmite nanofiber-PMSQ porous monolith acts as a high thermal insulator in low vacuum, and its application as an insulating material in vacuum environments is currently being investigated. However, the mechanism by which such core-shell structures are formed remains unclear, and boehmite nanofiber-silsesquioxane remains the only boehmite nanofiber-PMSQ reported to date. In this paper, nanofiber-reinforced macroporous monoliths

have been fabricated by using distributability during phase separation, with the aim of establishing a general method applicable to other composites.

Since boehmite nanofibers are stably dispersed in weak aqueous acid, the skeletal phase of the macroporous monolith can likely be formed through a polycondensation reaction by acid catalysis. In this report, a resorcinol-formaldehyde composite material with boehmite nanofibers was prepared by using an aqueous acetic acid condition[20] to prevent aggregation of nanofibers. The sample preparation procedure is as follows. (1) The boehmite nanofiber dispersion was diluted to x wt % with water and acetic acid to have an acetic acid concentration of 1 M. (2) Resorcinol ($2.2 \times y$ g) was dissolved in 8 mL of diluted boehmite nanofiber dispersion, then $3.0 \times y$ mL of 37 % formaldehyde aqueous solution was added. The mixture was stirred at room temperature for 10 min. (3) The resultant sol was poured into a sealed mold, then allowed to stand in a 60 °C oven for 12 h for gelation and aging. (4) The obtained gel was immersed in water and ethanol to remove unreacted reagents, then dried at 60 °C. The physical properties of the prepared samples, RB-x-y, are shown in Table 1. All the samples had macroporous structures, and the skeleton became finer due to the addition of boehmite nanofibers (Figures 1 and S1). This miniaturization of the skeletal structures occurred because a fixed amount of RF polymer phase attempted to exist around more nanofibers. The transmission electron microscope (TEM) images of the samples RB-x-2 in Figures 2a-d and S2 show boehmite nanofibers in the skeleton. No obvious bundle structures surround the boehmite nanofibers, and each fiber was individually dispersed within the resorcinol-formaldehyde skeletal phase. In the composition RB-0.23-2 with a low boehmite nanofiber concentration, the nanofibers are arranged in random directions within the framework of the monolith, whereas many nanofibers are aligned almost parallel to the skeleton about RB-3.6-2, RB-1.8-2, and RB-0.90-2 like plant stem (Figure 2e). Because boehmite nanofibers have a high aspect ratio with a length of micrometers, they likely align in parallel preferentially when the diameter of the skeleton becomes smaller than the length of the nanofibers. The bulk density and the porosity of the representative sample RB-3.6-2 were 0.27 g cm^{-3} and 82 %, respectively.

Table 1. Properties of the RF and the RF-boehmite nanofiber monoliths.

Sample RB-*x*-*y*	Nanofiber concentration of a sol [%]	Resorcinol [g]	37 % Formaldehyde [mL]	Bulk density [g cm^{-3}]	Porosity [%]	Young's modulus [MPa]	Thermal conductivity [mW m^{-1} K^{-1}]
RB-0-4	0	8.8	12.0	0.50	65	23.1	
RB-3.6-4	3.6	8.8	12.0	0.40	73	23.9	47.3
RB-1.8-4	1.8	8.8	12.0	0.41	72	24.3	
RB-0.90-4	0.90	8.8	12.0	0.40	71	25.4	
RB-0-2	0	4.4	6.0	0.28	81	1.07	49.7
RB-3.6-2	3.6	4.4	6.0	0.27	82	9.17	39.0
RB-1.8-2	1.8	4.4	6.0	0.27	81	10.2	42.4
RB-0.90-2	0.90	4.4	6.0	0.27	82	11.6	43.4
RB-0.23-2	0.23	4.4	6.0	0.42	72	10.4	49.9
RB-0-1	0	2.2	3.0	0.20	86	0.26	
RB-1.8-1	1.8	2.2	3.0	0.24	83	4.09	
RB-0.90-1	0.90	2.2	3.0	0.22	85	1.92	

In the RB-3.6-1 composition, the obtained gel became heterogeneous due to precipitation of the nanofibers.

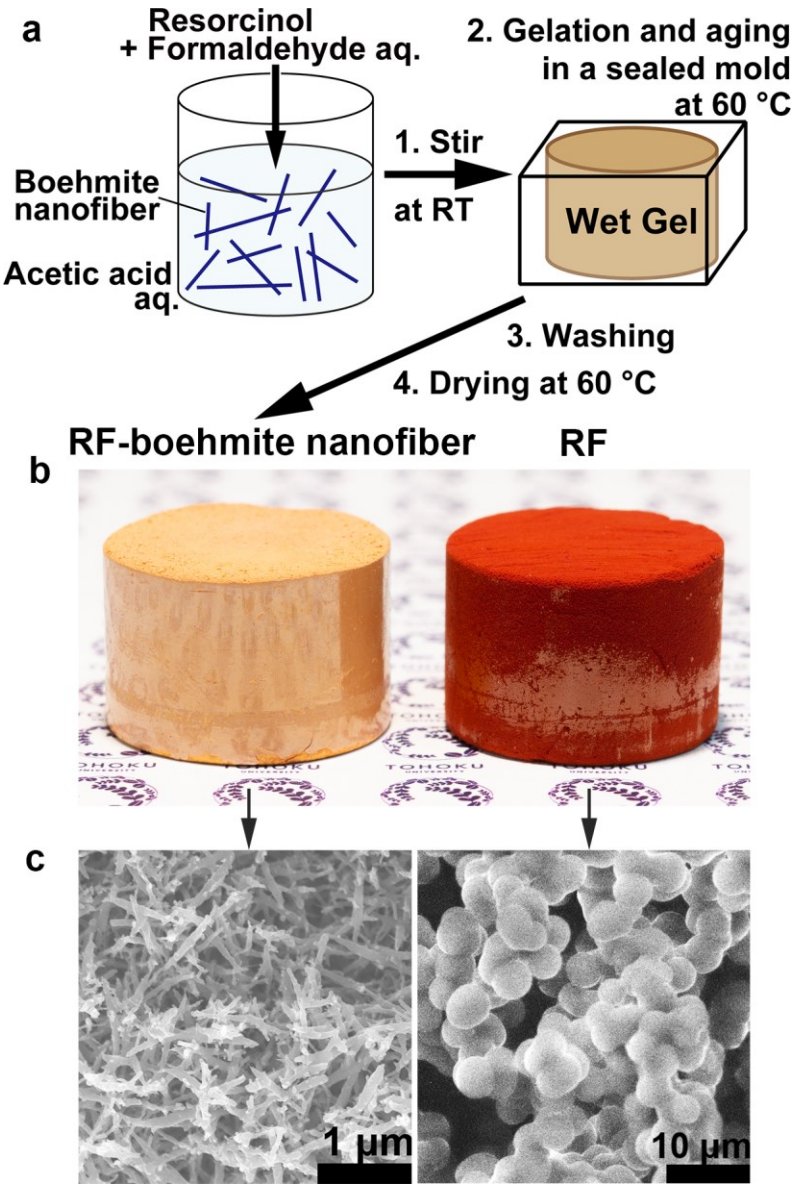

Figure 1. (a) Schematic image of the RF-boehmite nanofiber monolith preparation. (b) Photograph, and (c) scanning electron microscope (SEM) images of the RF-boehmite nanofiber and RF monoliths (RB-3.6-2 and RB-0-2, respectively). The diameter of the monoliths is about 26 mm. See also Figure S1 about samples RB-*x*-2.

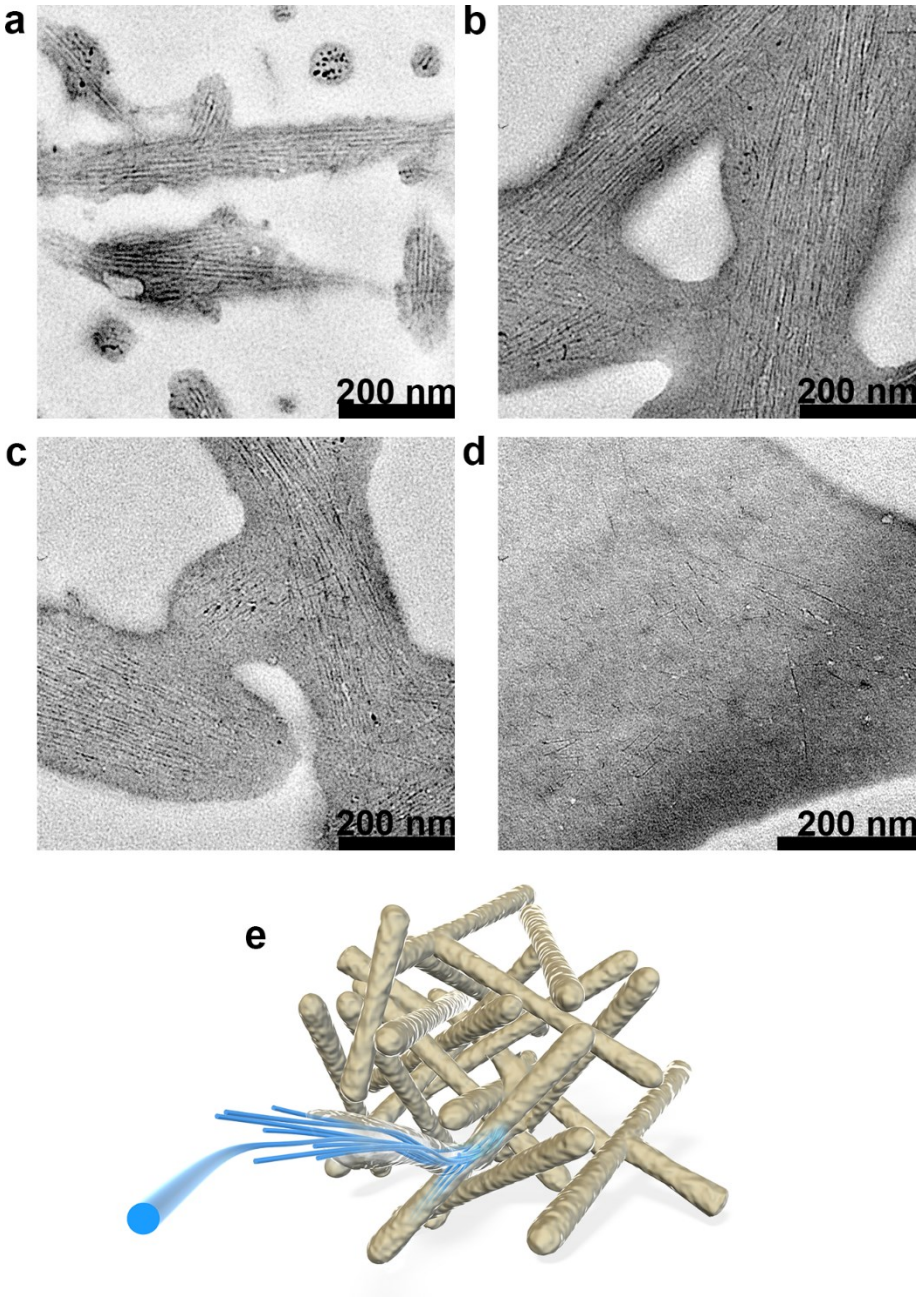

Figure 2. TEM images of RF-boehmite nanofiber monoliths (a) RB-3.6-2, (b) RB-1.8-2, (c) RB-0.90-2 and (d) RB-0.23-2 (the high-magnification image is shown in Figure S2), fabricated by changing the amount of boehmite nanofibers added. Boehmite nanofibers are aligned almost parallel to the skeleton in the samples RB-3.6-2, RB-1.8-2 and RB-0.90-2, while arranged in random in the composition RB-0.23-2. (e) Schematic diagram of the microstructure of RB-3.6-2 identified from the SEM and TEM images.

Generally, the structure of an anisotropic composite has higher strength than composites with a random structure. Figure 3 shows the relationship between the bulk density and the Young's modulus against uniaxial compression of RF and RF-boehmite nanofiber monoliths. The addition of boehmite nanofibers into the skeleton increased the Young's modulus for a given bulk density as compared with the case without the nanofibers, and all the samples recovered fully following a compression deformation of 5-10%. At $y = 1$ and 2, the existence of boehmite nanofibers increased the Young's modulus without significantly changing the bulk density, whereas the nanofibers made an effect of preventing syneresis during gelation and aging at $y = 4$. In the sparse skeletal RB-x-1 system, the effect of increasing the nanofibers also appeared due to low Young's modulus and fragility. As estimated from many other FRP materials, these mechanical properties are expected to be the result of the nanofiber reinforcement like plant stem structure, though the effect of morphological change cannot be excluded.[21-22] Future research including computer simulations may allow detailed evaluation of fiber reinforcement and finer control of the mechanical properties of monoliths.

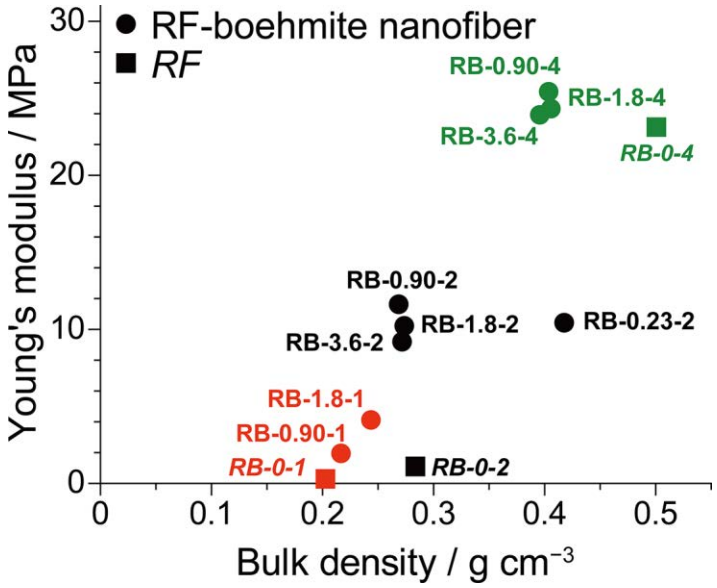

Figure 3. The relationship between bulk density and Young's modulus against uniaxial compression in RF and RF-boehmite nanofiber monoliths. Monoliths containing boehmite nanofibers had higher Young 's modulus concerning bulk density than just RF gels.

The morphologies of RF porous materials have previously been controlled by altering the fabrication conditions.[23-24] It has been reported that the thermal conductivity of low-bulk-density RF monoliths decreases upon appropriate control of the pore size, leading to research and development on RF monoliths as heat insulating materials.[25-27] When the thermal conductivity of the RF and RF-boehmite nanofiber monolithic panels RB-*x*-2 was measured at room temperature, the minimum one was 39 mW m^{-1} K^{-1} in the RB-3.6-2 composition with the smallest pore structure. This value is equivalent to high-performance glass wool insulation material. On the other hand, the thermal conductivity of RB-*x*-4 panels was high due to their higher bulk density, and the RB-*x*-1 panel was not practical because those panels were liable to collapse. In the case of Both phenolic resin and RF resin are flame resistant due to their molecular structure and thus can be used as heat-resistant/heat-shielding materials for space hardware applications.[28-30] If the thermal

capacity of RF resin is the same as that of phenolic resin 1.6 kJ kg^{-1} K^{-1}, then the thermal diffusivity of RB-3.6-2 was 0.9 m^2 s^{-1}. This value is close to that of heat resistant cork-phenol resin composites and carbon composites used for rocket components.[31-32] By optimizing the molecular structure of the resin in the skeletal phase, it can be expected that these composite materials will be further improved in the future. Flame resistance was also investigated by applying a liquefied natural gas (LNG) burner flame at ~ 1700 ° C to the RF-boehmite nanofiber monolith. (Figure 4, Movie S1). Although carbonization occurred gradually and the outermost surface cracked due to shrinkage, the monolith did not collapse, and the cylindrical shape did not change greatly even if a flame was applied for 10 min or longer. The boehmite contained in the skeleton undergoes a dehydration reaction at 300 °C and is transformed into alumina, and thus its combination with formaldehyde-phenolic resin should provide material useful for flame-resistant applications. Resorcinol-formaldehyde (RF)-boehmite nanofiber porous monoliths and their derivatives hold promise as materials for space development, such as in ablators used for thermal protection during atmospheric re-entry. In the future, we will prepare equipment and conduct tests at higher temperatures according to industry standards and actual use conditions.

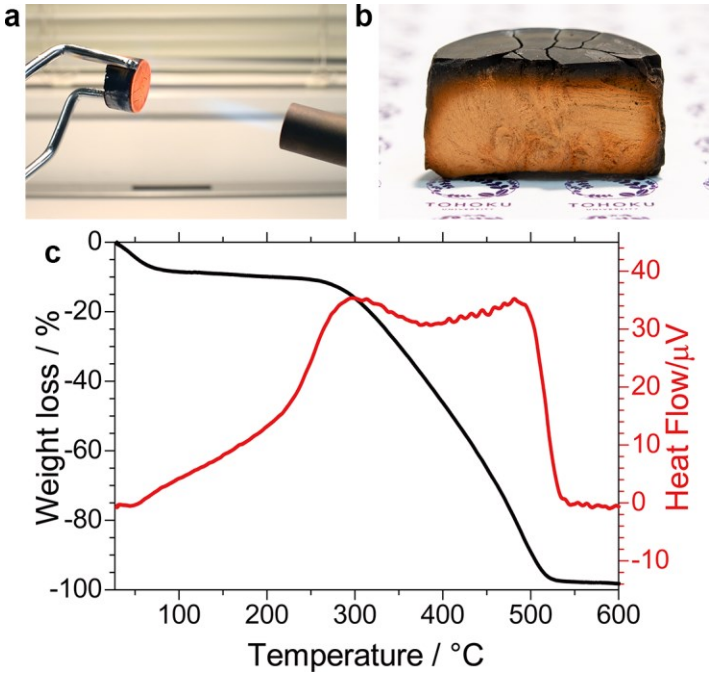

Figure 4. (a) Photographs of a flame resistance test on the RF-boehmite nanofiber monolith RB-3.6-2. The diameter of the monoliths is about 26 mm. (b) Cross-section photo of the resultant sample after 40 seconds exposure to flame. Only the surface was carbonized, and noticeable collapse had not occurred. See also Movie S1. (c) Thermogravimetric–differential thermal analysis (TG–DTA) curves of RF-boehmite nanofiber monolith RB-3.6-2 in the air. Since the content of nanofibers was much smaller than that of RF, the dehydration reaction peak (at ~300 °C)[16] of boehmite could not be distinguished from the DTA curve.

In summary, composite macroporous monoliths were fabricated by distributing nanofibers to the skeletal phase in RF porous structures formed by phase separation in an aqueous sol. The diameter of the composite skeleton decreased as the boehmite nanofiber concentration increased and the nanofibers were oriented parallel to the skeleton. The addition of a small amount of boehmite nanofibers increased the Young's modulus for compression. The composite monolithic panels exhibited a low thermal conductivity of 39 mW m^{-1} k^{-1} at a minimum and high flame retardance.

There have been few reports of methods for the preparation of porous monoliths reinforced with nanofibers inside the fine skeleton. The simple method for the formation of porous nanofiber-reinforced material is likely applicable to other resins, leading to another high-strength polymer monoliths and their applications in the future.

ASSOCIATED CONTENT

Supporting Information. The following files are available free of charge.

Experimental details, SEM images, and TEM images (PDF).

Movie of a flame resistance test on RB-3.6-1 (MPG).

AUTHOR INFORMATION

Corresponding Author

* Email: gen@aerogel.jp

Notes

The author declares no competing financial interest.

ACKNOWLEDGMENT

This research was supported by Japan Society for the Promotion of Science (JSPS) Grants-in-Aid for Scientific Research (KAKENHI, No. 17K14541).

REFERENCES

(1) Gibson, L. J.; Ashby, M. F. *Cellular Solids: Structure and Properties*, 2nd Edition ed.; Cambridge University Press: Cambridge, UK, 1999.

(2) Gesser, H. D.; Goswami, P. C. Aerogels and Related Porous Materials. *Chem. Rev.* **1989**, *89*, 765-788.

(3) Brinker, C. J.; Scherer, G. W. *Sol-Gel Science: The Physics and Chemistry of Sol-Gel Processing*, Academic Press: San Diego, 1990.

(4) Zhang, G.; Dass, A.; Rawashdeh, A.-M. M.; Thomas, J.; Counsil, J. A.; Sotiriou-Leventis, C.; Fabrizio, E. F.; Ilhan, F.; Vassilaras, P.; Scheiman, D. A.; McCorkle, L.; Palczer, A.; Johnston, J. C.; Meador, M. A.; Leventis, N. Isocyanate-Crosslinked Silica Aerogel Monoliths: Preparation and Characterization. *J. Non-Cryst. Solids* **2004**, *350*, 152-164.

(5) Meador, M. A. B.; Fabrizio, E. F.; Ilhan, F.; Dass, A.; Zhang, G.; Vassilaras, P.; Johnston, J. C.; Leventis, N. Cross-linking Amine-Modified Silica Aerogels with Epoxies: Mechanically Strong Lightweight Porous Materials. *Chem. Mater.* **2005**, *17*, 1085-1098.

(6) Guo, H.; Nguyen, B. N.; McCorkle, L. S.; Shonkwiler, B.; Meador, M. A. B. Elastic Low Density Aerogels Derived from Bis 3-(Triethoxysilyl)propyl Disulfide, Tetramethylorthosilicate and Vinyltrimethoxysilane via a Two-step Process. *J. Mater. Chem.* **2009**, *19*, 9054-9062.

(7) Kanamori, K.; Aizawa, M.; Nakanishi, K.; Hanada, T. New Transparent Methylsilsesquioxane Aerogels and Xerogels with Improved Mechanical Properties. *Adv. Mater.* **2007**, *19*, 1589-1593.

(8) Hayase, G.; Kugimiya, K.; Ogawa, M.; Kodera, Y.; Kanamori, K.; Nakanishi, K. The Thermal Conductivity of Polymethylsilsesquioxane Aerogels and Xerogels with Varied Pore Sizes for Practical Application as Thermal Superinsulators. *J. Mater. Chem. A* **2014**, *2*, 6525-6531.

(9) Hayase, G.; Kanamori, K.; Nakanishi, K. New Flexible Aerogels and Xerogels Derived from Methyltrimethoxysilane/Dimethyldimethoxysilane Co-precursors. *J. Mater. Chem.* **2011**, *21*, 17077-17079.

(10) Hayase, G.; Kanamori, K.; Fukuchi, M.; Kaji, H.; Nakanishi, K. Facile Synthesis of Marshmallow-like Macroporous Gels Usable under Harsh Conditions for the Separation of Oil and Water. *Angew. Chem., Int. Ed*. **2013**, *52*, 1986-1989.

(11) Hayase, G.; Ohya, Y. Marshmallow-like Silicone Gels as Flexible Thermal Insulators and Liquid Nitrogen Retention Materials and Their Application in Containers for Cryopreserved Embryos. *Appl. Mater. Today* **2017,** *9*, 560-565.

(12) Parmenter, K. E.; Milstein, F. Mechanical Properties of Silica Aerogels. *J. Non-Cryst. Solids* **1998,** *223*, 179-189.

(13) Li, L. C.; Yalcin, B.; Nguyen, B. N.; Meador, M. A. B.; Cakmak, M. Flexible Nanofiber-Reinforced Aerogel (Xerogel) Synthesis, Manufacture, and Characterization. *ACS Appl. Mater. Interfaces* **2009,** *1*, 2491-2501.

(14) Feng, J. Z.; Zhang, C. R.; Feng, J.; Jiang, Y. G.; Zhao, N. Carbon Aerogel Composites Prepared by Ambient Drying and Using Oxidized Polyacrylonitrile Fibers as Reinforcements. *ACS Appl. Mater. Interfaces* **2011,** *3*, 4796-4803.

(15) Li, Z.; Gong, L. L.; Cheng, X. D.; He, S.; Li, C. C.; Zhang, H. P. Flexible Silica Aerogel Composites Strengthened with Aramid Fibers and Their Thermal Behavior. *Mater. Des.* **2016,** *99*, 349-355.

(16) Hayase, G.; Nonomura, K.; Hasegawa, G.; Kanamori, K.; Nakanishi, K. Ultralow-Density, Transparent, Superamphiphobic Boehmite Nanofiber Aerogels and Their Alumina Derivatives. *Chem. Mater.* **2015,** *27*, 3-5.

(17) Hayase, G.; Funatomi, T.; Kumagai, K. Ultralow-Bulk-Density Transparent Boehmite Nanofiber Cryogel Monoliths and Their Optical Properties for a Volumetric Three-Dimensional Display. *ACS Appl. Nano Mater.* **2018,** *1*, 26-30.

(18) Nagai, N.; Mizukami, F. Properties of Boehmite and Al_2O_3 Thin Films Prepared from Boehmite Nanofibres. *J. Mater. Chem.* **2011,** *21*, 14884-14889.

(19) Hayase, G.; Nonomura, K.; Kanamori, K.; Maeno, A.; Kaji, H.; Nakanishi, K. Boehmite Nanofiber-Polymethylsilsesquioxane Core-Shell Porous Monoliths for a Thermal Insulator under Low Vacuum Conditions. *Chem. Mater.* **2016,** *28*, 3237-3240.

(20) Brandt, R.; Petricevic, R.; Probstle, H.; Fricke, J. Acetic Acid Catalyzed Carbon Aerogels. *J. Porous. Mater.* **2003,** *10*, 171-178.

(21) Pekala, R. W.; Alviso, C. T.; Lemay, J. D. Organic Aerogels: Microstructural Dependence of Mechanical Properties in Compression. *J. Non-Cryst. Solids* **1990,** *125*, 67-75.

(22) Woignier, T.; Reynes, J.; Alaoui, A. H.; Beurroies, I.; Phalippou, J. Different Kinds of Structure in Aerogels: Relationships with the Mechanical Properties. *J. Non-Cryst. Solids* **1998,** *241*, 45-52.

(23) Pekala, R. W. Organic Aerogels from the Polycondensation of Resorcinol with Formaldehyde. *J. Mater. Sci.* **1989,** *24*, 3221-3227.

(24) Al-Muhtaseb, S. A.; Ritter, J. A. Preparation and Properties of Resorcinol-Formaldehyde Organic and Carbon Gels. *Adv. Mater.* **2003,** *15*, 101-114.

(25) Lu, X.; Wang, P.; Arduinischuster, M. C.; Kuhn, J.; Buttner, D.; Nilsson, O.; Heinemann, U.; Fricke, J. Thermal Transport in Organic and Opacified Silica Monolithic Aerogels. *J. Non-Cryst. Solids* **1992,** *145*, 207-212.

(26) Lu, X.; Arduinischuster, M. C.; Kuhn, J.; Nilsson, O.; Fricke, J.; Pekala, R. W. Thermal Conductivity of Monolithic Organic Aerogels. *Science* **1992,** *255*, 971-972.

(27) Rey-Raap, N.; Calvo, E. G.; Menendez, J. A.; Arenillas, A. Exploring the Potential of Resorcinol-Formaldehyde Xerogels as Thermal Insulators. *Microporous Mesoporous Mat.* **2017,** *244*, 50-54.

(28) Vankrevelen, D. W. Some Basic Aspects of Flame Resistance of Polymeric Materials. *Polymer* **1975,** *16*, 615-620.

(29) Badhe, Y.; Balasubramanian, K. Novel Hybrid Ablative Composites of Resorcinol Formaldehyde as Thermal Protection Systems for Re-entry Vehicles. *RSC Adv.* **2014,** *4*, 28956-28963.

(30) Daniel, A.; Badhe, Y.; Srikanth, I.; Gokhale, S.; Balasubramanian, K. Laser Shielding and Thermal Ablation Characteristics of Resorcinol Formaldehyde/Boron Nitride Composites for Thermal Protection Systems. *Ind. Eng. Chem. Res.* **2016,** *55*, 10645-10655.

(31) Sato, Y.; Ohtake, K.; Shimada, T.; Sato, E. Evaluation of Thermal Diffusivity of Rocket Nozzle Materials. *Netsu Bussei* **2003,** *17*, 199-204.

(32) Aerospace | Materials & Applications > Amorim Cork Composites. https://amorimcorkcomposites.com/en-us/materials-applications/aerospace/. (accessed July 24th, 2018)